

Qualitative Estimation of the Single-Electron Transfer Step Energetics Mediated by Samarium(II) Complexes: A “SOMO–LUMO Gap” Approach

Christos E. Kefalidis,[†] Stéphanie Essafi,[‡] Lionel Perrin,^{†,§} and Laurent Maron^{*,†}

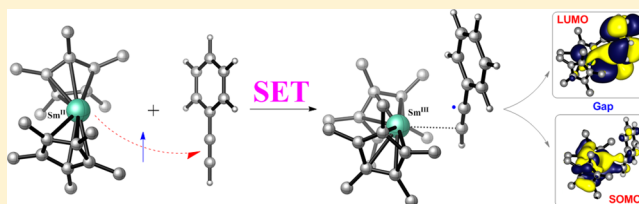
[†]Université de Toulouse et CNRS, INSA, UPS, CNRS, UMR 5215, LPCNO, 135 Avenue de Rangueil, F-31077 Toulouse, France

[‡]School of Chemistry and Centre for Computational Chemistry, University of Bristol, Cantock's Close, Bristol BS8 1TS, United Kingdom

S Supporting Information

ABSTRACT: Lanthanide II organometallic complexes usually initiate reactions via a single-electron transfer (SET) from the metal to a bonded substrate. Extensive mechanistic studies were carried out for lanthanide III complexes in which no change of oxidation state is involved. Some case-dependent strategies were reported by our group in order to account for a SET event in organometallic computed studies. In the present study, we show that analysis of DFT orbital spectra allows

differentiating between exothermic and endothermic electron transfer. This methodology appears to be general; it allows differentiating between lanthanide centers and substituent effects on metallocenes. For that purpose, we considered mainly various samarocene adducts as well as a SmI₂ complex explicitly solvated by THF. Comparison between DFT methods and *ab initio* (CAS-SCF and HF) computational level revealed that the SOMO–LUMO gap computed at the DFT B3PW91 level, in combination with small-core RECPs and standard basis sets, offers a qualitative estimation of the energetics of the SET that is in line with both CAS-SCF calculations and experimental results when available. This orbital-based approach, based on DFT calculation, affords a fast and efficient methodology for pioneer exploration of the reactivity of lanthanide(II) mediated by SET.



INTRODUCTION

Reactivity of divalent lanthanide and trivalent actinides toward small molecules has regained attention in the past few years, mainly because there is a need for strong reducing agents that can activate selectively small organic molecules¹ and challengingly initiate CO₂ transformation under mild conditions.^{2–5} This chemistry is known to involve redox transformation by means of single-electron transfer (SET) from the f-element center to the substrate. Although this chemistry is well documented experimentally, there is a lack of understanding at the atomic level that could be filled by theoretical studies. So far, computational approaches have shown their ability in dealing with the reactivity of the f-element as long as no change in oxidation states is involved in the reactivity. Theoretical chemists have derived profit from this peculiarity by using large-core RECPs in which the f-shell belongs to the core of the atomic pseudopotential.⁶

Pioneer works on redox chemistry of uranium complexes (mainly uranyl) have shown that multireference and spin–orbit calculations were mandatory to represent their redox properties.^{7–10} However, such a methodology is not tractable for realistic organolanthanide chemical models that include more than 150 atoms. It is thus of interest to define and test alternative computational strategies in order to estimate SET energies. Booth et al.^{11–13} have shown that in Cp*₂Yb(2,2′-bipyridine) and Cp*₂Yb(1,10-phenanthroline) (Cp* = η⁵-

C₅Me₅), CAS-SCF calculations are required to describe the open-shell singlet ground state of these molecular complexes. Such calculations are not always manageable when studying the reactivity of f-element complexes since they often involve bimetallic species. More qualitative strategies have to be developed to assess the SET energetics within a realistic computational effort. In particular, it is of interest to rapidly know whether the SET is a critical step (i.e., endo- or exothermic). In that perspective, our group reported that DFT-based determination of the SET energy in Ln(II) chemistry with CO₂ is possible by taking advantage of the first-order Jahn–Teller effect induced by the reduction of CO₂.¹⁴ However, this approach failed to be general, and alternatives strategies were then envisaged to compute SET energies. We reported that DFT calculations can discriminate the propensity of cyclopentadienyl- and phospholythulium(II) complexes to transfer an electron toward pyridine as a ligand.¹⁵ In this study, we predicted that samarium(II) complexes should follow a similar trend to that of thulium, but the calculations were less straightforward. In order to describe the electron transfer from samarium(II) to pyridine, we had to consider an indirect assessment of the SET based on an isodesmic Born–Haber-type thermodynamic cycle. This scheme was previously applied

Received: November 13, 2013

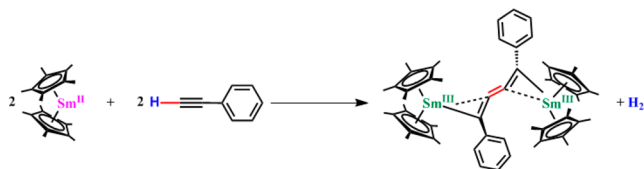
Published: March 12, 2014

with success in the investigation of the reactivity of uranium(III) complexes with various alkynes.¹⁶

The diversity of computational approaches suggests a need for a more general and straightforward method that will allow determining, at least, the sign and the range of the SET energy in lanthanide(II) complexes. In this contribution, we will show that the analysis of the DFT orbital spectra of Sm(II)–substrate adducts leads to a qualitative approximation of the SET energy. Indeed, for this combination of functional (B3PW91) and basis sets (see Computational Details), systematic errors are not large and allow us to have access to the correct sign of the SET energy. This will be demonstrated by comparing selected cases in which CAS-SCF calculations were performed. This straightforward and easy-to-handle strategy enables one to discriminate between reactions that could be controlled by the SET or by subsequent reactivity.

RESULTS AND DISCUSSION

Alkyne Dimerization Catalyzed by Cp*₂Sm. Experimentally, Evans' group reported that phenylacetylene dimerizes in the presence of Cp*₂Sm(THF)_{0.2} (where Cp* = C₅Me₅).^{17,18} This reaction (eq 1) yields a bimetallic samarium(III) complex, implying the reduction of the two phenylacetylene molecules by two single-electron transfer steps.



In the aforementioned reaction, a SET from one *f*-occupied orbital of the samarium(II) to the π^* of phenylacetylene is taking place. DFT geometry optimization (B3PW91) of the septet spin state was initially carried out on Cp*₂Sm(η^2 -HCCPh). Both the optimized geometry and NBO/NPA analyses were in line with a neutral substrate and a Sm(II)-type core in which six unpaired electrons are localized. As no Jahn–Teller distortion is observed, the Born–Haber cycle approach was then used to determine the SET energy.^{14,15} This computational scheme leads to an endergonic SET by 7.0 kcal mol⁻¹. To further validate this energy, the SET energy was also estimated via the optimization of the quintet spin state of the phenylacetylene adduct in which the π^* orbital of the alkyne ligand is forced to be occupied. The diabatic difference between the septet and the quintet affords another estimation of the SET energy, which is 12.7 kcal mol⁻¹. However, this value has the same sign and lies in the same range as the one obtained by the indirect method based on a Born–Haber cycle. At this point, in order to further validate the computed DFT SET energy, we turned our attention to more sophisticated and higher level calculations. For that purpose, CAS-SCF calculations were carried out by distributing six electrons in eight orbitals ($7f + \pi^*$). It is noteworthy that similar active spaces were successfully used in ytterbium chemistry to discriminate between the open-shell singlet and triplet as a putative electronic ground state.^{11–13} In particular, these high-level *ab initio* calculations were performed on the DFT geometry obtained for the septet spin state. The lowest root corresponds to an $f^5-\pi^{*1}$ occupation, whereas the second root corresponds to an f^6 occupation. This indicates that the lowest septet spin state can be interpreted as a complex in which the

coordinated substrate is monoreduced. At this level of theory, the SET energy is estimated to be -78.6 kcal mol⁻¹, which is significantly different from the one obtained at the DFT level. The origin of this discrepancy was investigated by analyzing the nature of the restricted open-shell Hartree–Fock (ROHF) orbitals used as a guess function for the CAS-SCF calculations. Unexpectedly, analysis of the spectrum of molecular orbitals (MO) shows that the π^* orbital of the alkyne ligand is already occupied, whereas the f_σ orbital is unoccupied.¹⁹

As a result, the phenylacetylene is reduced at the HF level. This indicates that the reduction already occurs upon coordination of the substrate to the metal center. The energy gap between the aforementioned two orbitals is 88.7 kcal mol⁻¹, within the range of the SET energy computed at the CAS-SCF level (negative sign of the SET energy). A similar analysis was carried out on Kohn–Sham MOs. The π^* orbital of the alkyne turned out to be occupied in the septet state, and the LUMO involves the π^* orbital of the ligand (Figure 1).

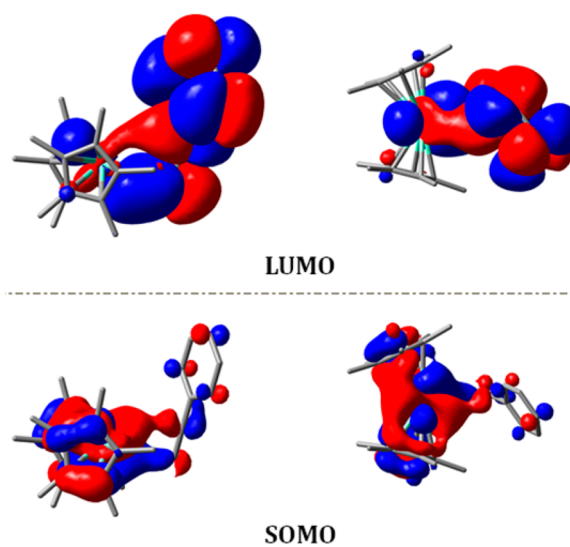


Figure 1. Top and side views of DFT-B3PW91 LUMO (top) and SOMO (bottom) orbitals of the Cp*₂Sm(HCCPh) complex.

Likewise at the DFT level, the phenylacetylene in Cp*₂Sm(HCCPh) is reduced, although the nature of the SOMO and the LUMO is unclear, as they both involve the π^* orbital of the phenylacetylene. In fact, the difference in the nature of the LUMO is due to the PW91 correlation functional in the DFT approach. Indeed, decreasing the amount of correlation, going hence to a spin-polarized local density approximation (LDA-SWN), changes the nature of the LUMO. The latter is now the same as at the HF level, in which the π^* orbital remains occupied as a SOMO (Figure 2).

The electronic structure of Cp*₂Sm(η^2 -HCCPh) and its chemical interpretation can be extracted from CAS-SCF calculations. The canonical orbitals of the active space display a mixing between a π^* orbital (SOMO) and a $4f$ one (LUMO), as in the DFT (B3PW91) calculation. A relatively important degree of mixing (62% *f*, 38% π^*) is found though. This demonstrates that the mixture is at least partially attributed to the inclusion of electron correlation either explicitly (CAS-SCF) or implicitly (DFT). As a result, DFT calculations qualitatively reproduce CAS-SCF bonding descriptions, but the sign of the SET energy computed by DFT using the different methodology above is not correct. Moreover, the direct

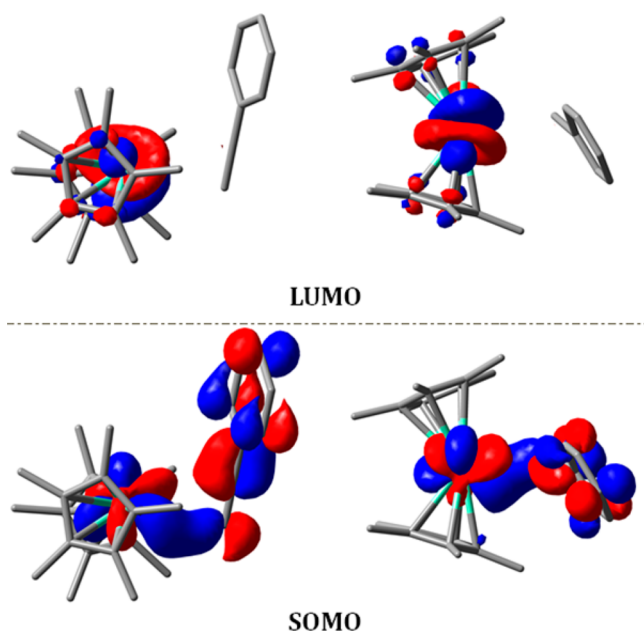


Figure 2. Top and side views of DFT-LDA LUMO (top) and SOMO (bottom) orbitals of the $\text{Cp}^*_2\text{Sm}(\text{HCCPh})$ complex.

estimation of the SET energy via the optimization of the quintet spin state is not a good approximation in this case. Indeed, a CAS-SCF benchmark calculation reveals that the quintet spin state is $97.0 \text{ kcal mol}^{-1}$ higher in energy than the lowest septet and therefore $19.4 \text{ kcal mol}^{-1}$ higher than the other septet (nonreduced metal adduct). This energy matches the SET energy computed using this quintet at the DFT level, indicating that the quintet is a high-energy excited state. Finally, the SOMO–LUMO energy gap at the DFT (B3PW91) level of the septet spin state was estimated, where the π^* was already occupied, being $32.4 \text{ kcal mol}^{-1}$, in the same direction as the CAS-SCF SET energy (both are negative).

In order to highlight the impact that the π conjugation has on the SET, we considered the reactivity of $\text{Cp}^*_2\text{Sm}(\text{II})$ toward an aliphatic alkyne (hex-1-yne). As in the phenylacetylene case, a geometry optimization of the hex-1-yne adduct in a septet spin state was carried out. However, the estimation of the SET energy based on DFT was not carried out before analyzing the MO spectrum and performing the CAS-SCF calculations. Once again, at the HF level, five $4f$ orbitals are singly occupied as well as the alkyne π^* orbital, while the LUMO corresponds mainly to a $4f$ orbital. In this case, the LUMO is not a pure $4f$, as some contributions of the π^* are apparent. This again indicates that hex-1-yne is already reduced upon coordination to the $\text{Sm}(\text{II})$ center, being the same as in the phenylacetylene example. By using the same active space as in the previous case, the SET energy is computed to be $-39.9 \text{ kcal mol}^{-1}$, which is almost half of the energy compared to the phenylacetylene one. This decrease can be mainly attributed to the lack of conjugation in the hex-1-yne, which possesses a π^* orbital that is higher in energy with respect to the phenylacetylene case. Interestingly, the SOMO–LUMO gap at the HF level is $49.0 \text{ kcal mol}^{-1}$, in relative good agreement with the CAS-SCF value (negative sign for the SET energy). Similarly, the SOMO–LUMO gap at the DFT level is $62.8 \text{ kcal mol}^{-1}$ (negative sign for the SET energy). The shapes of the frontier orbitals are similar to those found at the HF level but with a greater degree of mixture, which is again consistent with the inclusion of the electron

correlation. This DFT-based orbital approach consequently seems to work as well for the mono-electron reduction of hex-1-yne by a $\text{Sm}(\text{II})$ precursor. At this stage, the full mechanism of hex-1-yne dimerization was computed, and a plausible enthalpy profile is given in the Supporting Information. Even though it is not the scope of this theoretical study, the overall reaction mechanism, involving bimetallic intermediates, is predicted to be kinetically easily accessible (activation barriers around $15.0 \text{ kcal mol}^{-1}$) and thermodynamically favorable.

To contrast with the alkyne dimerization obtained with $\text{Cp}^*_2\text{Sm}(\text{II})$, calculations were carried out on the experimentally reported reaction between $\text{Cp}^*_2\text{Eu}(\text{II})$ and HCCPh in THF.²⁰ In this study, Boncella et al. reported that, instead of a C–C coupling reactivity, the formation of the dimeric complex $[\text{Cp}^*_2\text{Eu}(\mu\text{-CCPh})(\text{THF})_2]_2$ occurs after the formal loss of one HCp^* molecule from each europium center. The latter most probably remains in its low-oxidation state (II) throughout the process. A close inspection of the frontier orbitals of $\text{Cp}^*_2\text{Eu}(\text{HCCPh})$ computed at the DFT level confirms that no SET is occurring in this case (Figure 3).

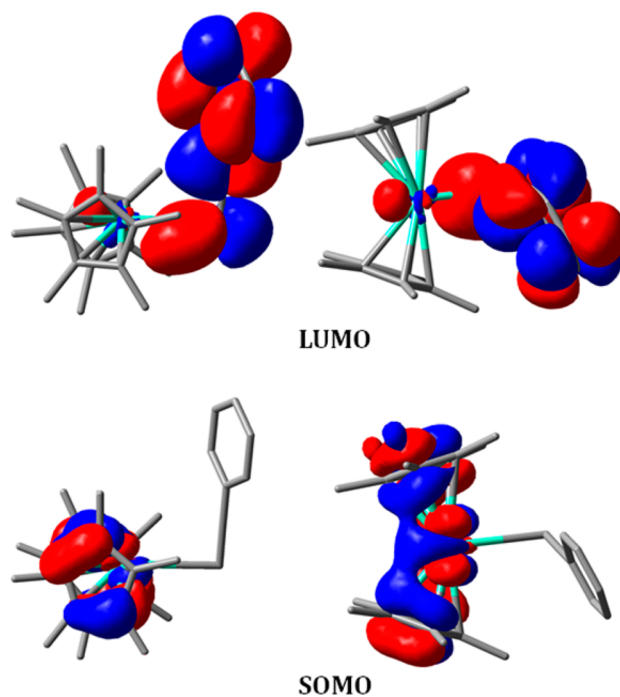


Figure 3. Top and side views of DFT-B3PW91 LUMO (top) and SOMO (bottom) orbitals of the $\text{Cp}^*_2\text{Eu}(\text{HCCPh})$ complex.

In $\text{Cp}^*_2\text{Eu}(\text{HCCPh})$, the SOMO corresponds to a pure $4f$ orbital and the LUMO is mainly an alkyne π^* orbital. This shows that the SET is not induced by coordination of the incoming alkyne. This is in line with the interpretation of the experimental observations. In terms of energies, the DFT SOMO–LUMO gap of $48.3 \text{ kcal mol}^{-1}$ (positive sign) is coherent with a lack of SET and explains the type of reactivity observed. Therefore, this simple and easy-to-handle methodology is able to reproduce adequately subtle differences in terms of electron configuration between $\text{Sm}(\text{II})$ and $\text{Eu}(\text{II})$ that result in distinct reactivity.

Coordination-Induced SET. Inspired by the seminal work of Andersen's group on coordination of bipyridine and phenanthroline to Cp^*_2Yb ,^{21,22} the coordination chemistry of bipyridine (2,2'-bipyridine), acridine (9-azaanthracene), and

terpyridine (2,6-bis(2-pyridyl)pyridine) to the Cp^*_2Sm complex has been investigated. In particular, it has been shown that the coordination of bipyridine²³ and terpyridine²⁴ leads to Sm^{III} -substrate complexes in which the ground-state configuration is $4f^5-\pi^*$, whereas coordination of acridine leads to a Sm^{III} -acridine-acridine- Sm^{III} complex.

Following the same strategy as for alkyne dimerization, CAS-SCF calculations were carried out on the DFT-optimized structures. In order to avoid discussion on the correlation energy consistency, the same active space was defined for all systems compared to the alkyne dimerization: six electrons distributed in seven orbitals ($6f + \pi^*$). Interestingly, unlike the alkyne complexes reported in the previous section, the samarium centers in these complexes are found not to be reduced/oxidized at the HF level. Nevertheless, CAS-SCF calculations clearly indicate that the $f^5-\pi^*$ configuration is the lowest in energy and predict a coordination-induced SET. More specifically, in the bipyridine complex, the $f^6-\pi^{*0}$ state is 22.5 kcal mol^{-1} higher in energy than the $f^5-\pi^*$ state. This SET energy is close to the one computed for the hex-1-yne complex. DFT (B3PW91) orbitals were analyzed. As in the alkyne complexes, the SOMO and LUMO orbitals strongly involve the π^* of the bipyridine (Figure 4). This indication points out

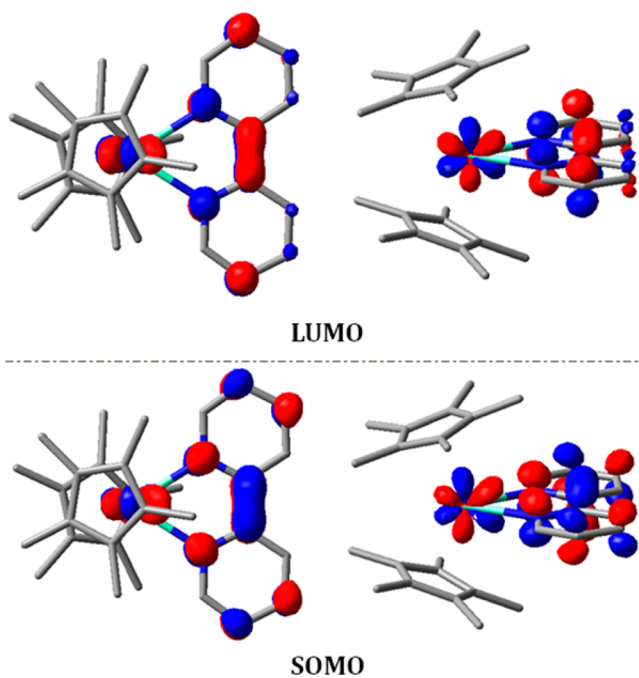


Figure 4. Top and side views of DFT-B3PW91 LUMO (top) and SOMO (bottom) orbitals of the $\text{Cp}^*_2\text{Sm}(\text{bipy})$ complex.

clearly that the system is already reduced at the DFT level, with the SOMO–LUMO gap being 28.9 kcal mol^{-1} (negative sign for the SET energy). This value is in good agreement with the CAS-SCF one, indicating that the simple orbital-based approach is still valid in this case. Applying this strategy to the acridine and terpyridine samarium complexes leads to similar results. For the acridine, the CAS-SCF calculations also predict the coordination-induced SET behavior with an energy of $-23.9 \text{ kcal mol}^{-1}$. The frontier orbitals computed at the DFT level (Figure 5) are compatible with a reduced/oxidized system in which a SOMO–LUMO energy gap of 22.4 kcal mol^{-1} is computed (negative sign for the SET energy). This is in

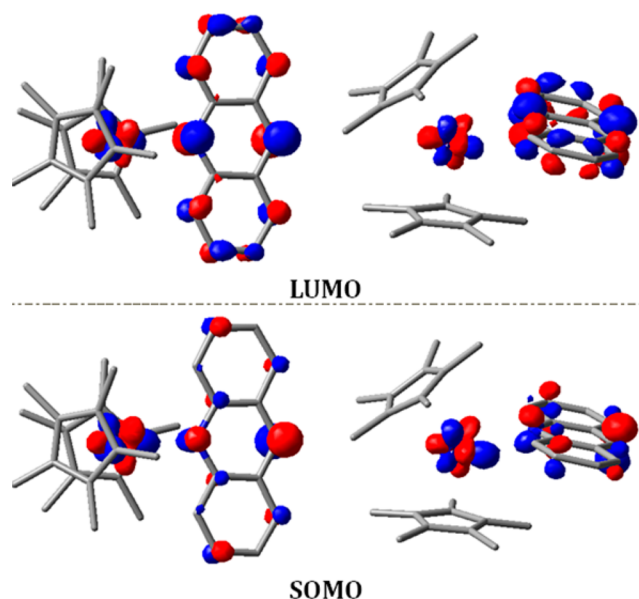


Figure 5. Top and side views of DFT-B3PW91 LUMO (top) and SOMO (bottom) orbitals of the $\text{Cp}^*_2\text{Sm}(\text{acridine})$ complex.

excellent agreement with the energy gap estimated at the CAS-SCF level.

For the terpyridine complex, only the DFT analysis was carried out because the system closely resembles the bipyridine system, but with a more extended π conjugation. We thus expect an easier SET process than for bipyridine. The DFT frontier orbitals presented in Figure 6 involve again participation of the π^* and are thus compatible with a reduced/oxidized compound. Moreover, a closer look at the orbital coefficients demonstrates that the π^* is more involved in

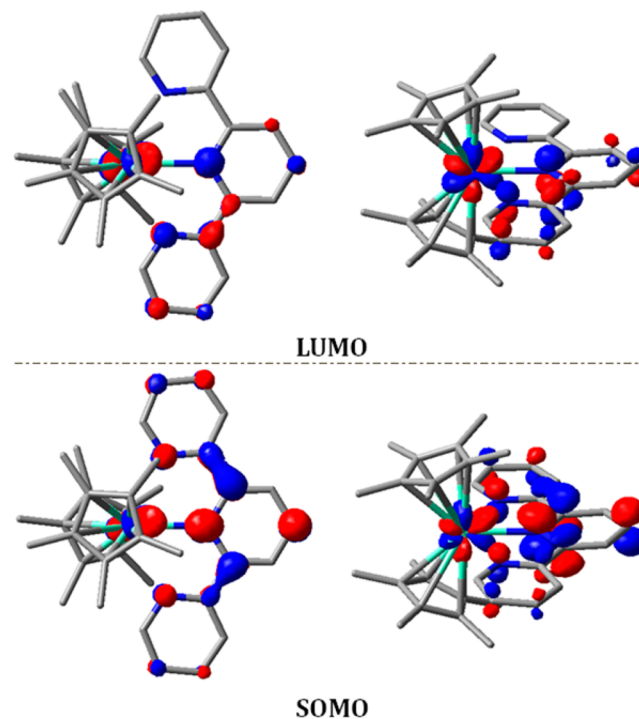


Figure 6. Top and side views of DFT-B3PW91 LUMO (top) and SOMO (bottom) orbitals of the $\text{Cp}^*_2\text{Sm}(\text{tpy})$ complex.

the SOMO than in the LUMO orbital, reminiscent of the situation found in the phenylacetylene complex. Therefore, a lower energy SOMO–LUMO gap is found, being 30.5 kcal mol⁻¹ (negative sign for the SET energy), in line with an easier SET process for terpyridine than for bipyridine.

In a recent report, Nocton et al. demonstrated that the replacement of the ancillary Cp* ligand by the bulkier Cp' (where Cp' = 1,2,4'-Bu₃C₅H₂) induces a drastic change in reactivity of Cp'₂Sm toward pyridine.²⁵ Indeed, rather than the coupling between the two pyridines in their 4,4'-position,²⁶ the formation of a pyridine monoadduct has been observed. This difference in reactivity can serve as an additional test to confirm the relevancy of our computational strategy. For that purpose, the Kohn–Sham orbitals were computed at the B3PW91 level, and the highest occupied and unoccupied ones are depicted in Figure 7.

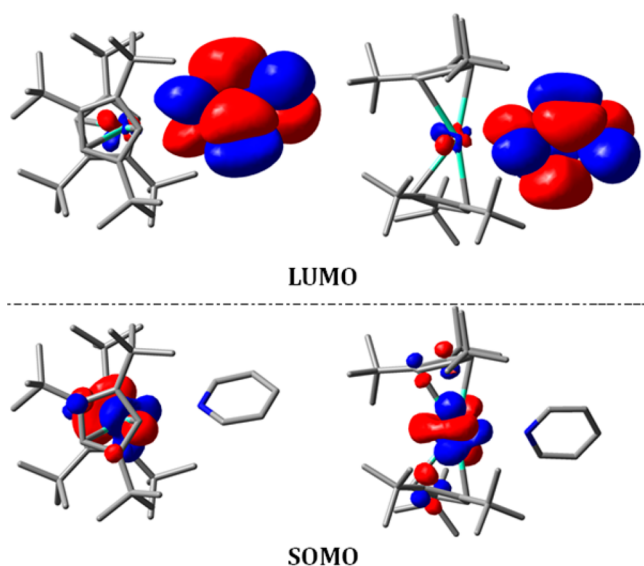


Figure 7. Top and side views of DFT-LDA LUMO (top) and SOMO (bottom) orbitals of the Cp'₂Sm(py) complex.

As in the case of the europium(II) complex reported above, the SOMO is a pure 4f orbital and the LUMO a π*. This supports an absence of SET in Cp'₂Sm(pyridine), which is in line with experimental reports. The DFT SOMO–LUMO gap is 36.9 kcal mol⁻¹ (positive sign for the SET energy). As a result, our methodology is also able to reproduce substituent effects of the cyclopentadienyl ligands.

SET in SmI₂ Chemistry. In order to further test our strategy, a different type of Sm(II) complex has been considered. Among all complexes used experimentally, samarium diiodide (SmI₂) is one of the most popular and commonly used in a variety of polar solvents, such as THF.^{27–29} However, studying theoretically its reactivity is a challenge, as various additives, such as hexamethylphosphoric amide (HMPA), are needed to increase SmI₂ reactivity/selectivity and determine the speciation of active complexes.^{29,30} Various experimental groups have indeed quantified the effect of HMPA on the redox potential of samarium(II) by studying the electrochemical behavior of, for instance, SmI₂/HMPA mixtures in various proportions.^{31–33} It was also shown experimentally that the reduction of ketone substrates by SmI₂(THF)_n was occurring upon coordination. So far, almost no theoretical studies dealt with such reactivity, apart from a

recent theoretical study by our group.³⁴ In this study it was demonstrated that theoretical approaches are now able to deal with the structural and, to a lesser extent, with the reactivity aspects of this highly reducing agent.

The initial step involved in the reactivity of SmI₂ toward ketones is the coordination, and we considered SmI₂(THF)₄(Ph₂CO) as a prototype complex. The analysis of the DFT frontier orbitals of SmI₂(THF)₄(Ph₂CO) (Figure 8) indicates that the carbonyl π* orbital is involved in both the

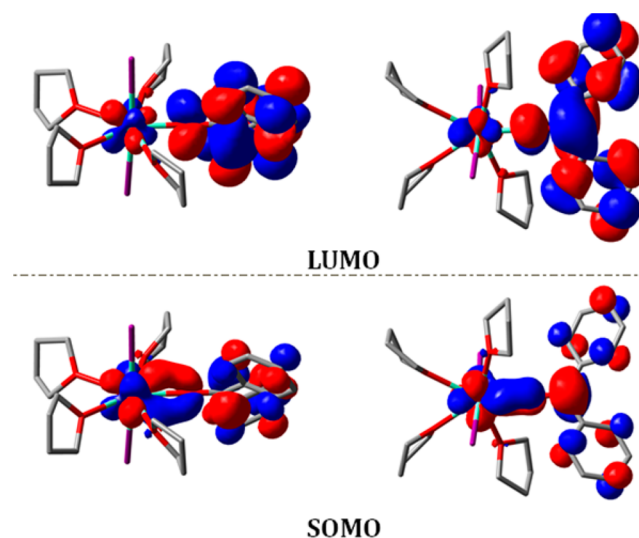


Figure 8. Top and side views of DFT-B3PW91 LUMO (top) and SOMO (bottom) orbitals of the SmI₂(THF)₄(Ph₂CO) complex.

SOMO and the LUMO of the system. This is similar to the systems that were reported in the two previous sections, and one can conclude a coordination-induced SET system. The SOMO–LUMO gap is computed to be 25.2 kcal mol⁻¹ (negative sign for the SET energy), in line with the electrochemical observations.³⁵ Thus, this very simple approach seems to work also in this case. This can be considered as a breakthrough in the theoretical treatment of the reactivity of divalent lanthanide complexes and opens a new area of investigation, especially for the reactivity promoted by the SmI₂ system.

CONCLUSION

In this study, the SET energy in samarium(II) redox chemistry with alkyne (phenylacetylene, hex-1-yne) and heteroaromatic compounds has been estimated using a variety of theoretical methods. In this regard, multiconfigurational methods (CAS-SCF) were used, and the estimated SET energies were compared to DFT values. The apparent “failure” of DFT was analyzed, and it was found that in these systems the substrates were already reduced upon coordination. This has been further highlighted by checking the MO spectra at both the HF and DFT (B3PW91) levels. In most of the cases, it was found that the π* of the substrate was occupied and that a 4f orbital was in fact the LUMO, in line with a partially reduced substrate, leading to an incorrect sign of the determined SET energy. This issue has been bypassed, by the use of the “SOMO–LUMO gap” approach. The latter allowed us to correctly determine the sign and even to estimate the SET energy at both the HF and DFT level. In addition, this approach was found to be in reasonable agreement with CAS-SCF results. Finally, this

method, which is simple and easy-to-handle, appears to be powerful toward the prediction of the reductive ability of samarium(II) organometallic and inorganic complexes. This was even extended to explain other reactivity mediated by other low-valent lanthanide complexes such as europocene(II). We have also shown that our methodology is able to account for the subtle substituent effects within the metallocene fragment. We believe that this computational approach can be generalized to other lanthanide metals and, thus, will allow us to focus on the ensuing reactivity involving monometallic or bimetallic complexes. Computational mechanistic studies of the dimerization of acridine by samarium(II) complexes as well as the dimerization of alkyne or the reactivity of SmI_2 toward different organic substrates are under way.

■ COMPUTATIONAL DETAILS

Calculations were performed with the GAUSSIAN 03 suite of programs.³⁶ Density functional theory (DFT) was applied by means of the B3PW91 hybrid functional.³⁷ For the lanthanide centers, the small-core RECP developed by the Stuttgart–Köln group was chosen and used in combination with their optimized valence basis sets.³⁸ Iodine atoms were represented by means of Stuttgart–Dresden effective core potentials in association with its basis set,³⁹ augmented by a d-polarization function ($\alpha = 0.730$).⁴⁰ The 6-31G(d,p) basis set was used for all other atoms. Geometry optimizations were performed on the full experimental systems without any symmetry constraints. The stationary points were characterized by full vibration frequency calculations. In all cases, the spin contamination has been checked and found to be small. Single-point multireference CAS-SCF calculations based on restricted open-shell canonical SCF orbitals were performed on the DFT-optimized geometries using the same basis set. Two active spaces were used: either an active space that involves six electrons in eight orbitals, i.e., all the Sm 4f orbitals and the lowest vacant π^* orbital on the substrate, or an active space that implies distribution of six electrons in seven orbitals; the lowest energy f orbital was not included in that case. Throughout the text the energies that have been used are the electronic ones, ΔE , in order to be in line with those obtained from CAS-SCF calculations.

■ ASSOCIATED CONTENT

Supporting Information

This material is available free of charge via the Internet at <http://pubs.acs.org>.

■ AUTHOR INFORMATION

Corresponding Author

*E-mail: laurent.maron@irsamc.ups-tlse.fr. Phone: 335 6155 9664. Fax: 335 6155 9697.

Present Address

[§] Institut de Chimie et Biochimie Moléculaires et Supramoléculaires, Université Lyon 1, CNRS UMR 5246,43 Boulevard du 11 Novembre 1918, F-69622 Villeurbanne, France.

Notes

The authors declare no competing financial interest.

■ ACKNOWLEDGMENTS

ANR, CNRS, and UPS are acknowledged for financial support. The authors thank CALMIP and CINES for a generous grant of computing time. L.M. is a member of the Institute Universitaire de France. L.M. would also like to thank the Humboldt Foundation.

■ REFERENCES

- (1) See for instance the entire volume of *Eur. J. Inorg. Chem.* **2013**, 22–23.
- (2) Bart, S. C.; Anthon, C.; Heinemann, F. W.; Bill, E.; Edelstein, N. M.; Meyer, K. *J. Am. Chem. Soc.* **2008**, *130*, 12536–12546.
- (3) Castro-Rodriguez, I.; Meyer, K. *J. Am. Chem. Soc.* **2005**, *127*, 11242–11243.
- (4) Summerscales, O. T.; Frey, A. S. P.; Cloke, F. G. N.; Hitchcock, P. B. *Chem. Commun.* **2009**, 198–200.
- (5) Frey, A. S. P.; Cloke, F. G. N.; Coles, M. P.; Maron, L.; Davin, T. *Angew. Chem., Int. Ed.* **2011**, *50*, 6881–6883.
- (6) Maron, L.; Eisenstein, O. *J. Phys. Chem. A* **2000**, *104*, 7140–7143.
- (7) La Macchia, G.; Infante, I.; Raab, J.; Gibson, J. K.; Gagliardi, L. *Phys. Chem. Chem. Phys.* **2008**, *10*, 7278–7283.
- (8) Gagliardi, L.; Roos, B. O. *Chem. Phys. Lett.* **2000**, *331*, 229–234.
- (9) Clavaguera-Sarrio, C.; Vallet, V.; Maynau, D.; Marsden, C. J. *J. Chem. Phys.* **2004**, *121*, 5312–5321.
- (10) Maron, L.; Leininger, T.; Schimmelpfennig, B.; Vallet, V.; Heully, J. L.; Teichteil, C.; Gropen, O.; Wahlgren, U. *Chem. Phys.* **1999**, *244*, 195–201.
- (11) Booth, C. H.; Walter, M. D.; Kazhdan, D.; Hu, Y.-J.; Lukens, W. W.; Bauer, E. D.; Maron, L.; Eisenstein, O.; Andersen, R. A. *J. Am. Chem. Soc.* **2009**, *131*, 6480–6491.
- (12) Booth, C. H.; Kazhdan, D.; Werkema, E. L.; Walter, M. D.; Lukens, W. W.; Bauer, E. D.; Hu, Y.-J.; Maron, L.; Eisenstein, O.; Head-Gordon, M.; Andersen, R. A. *J. Am. Chem. Soc.* **2010**, *132*, 17537–17549.
- (13) Nocton, G.; Booth, C. H.; Maron, L.; Andersen, R. A. *Organometallics* **2013**, *32*, 1150–1158.
- (14) Labouille, S.; Nief, F.; Maron, L. *J. Phys. Chem. A* **2011**, *115*, 8295–8301.
- (15) Labouille, S.; Nief, F.; Le Goff, X.-F.; Maron, L.; Kindra, D. R.; Houghton, H. L.; Ziller, J. W.; Evans, W. J. *Organometallics* **2012**, *31*, 5196–5203.
- (16) Kosog, B.; Kefalidis, C.; Heinemann, F. W.; Maron, L.; Meyer, K. *J. Am. Chem. Soc.* **2012**, *134*, 12792–12797.
- (17) Evans, W. J.; Keyer, R. A.; Ziller, J. W. *Organometallics* **1990**, *9*, 2628–2631.
- (18) Evans, W. J.; Keyer, R. A.; Ziller, J. W. *Organometallics* **1993**, *12*, 2618–2633.
- (19) As it was shown in our previous studies dealing with 4f elements, to reach the convergence on the correct spin state, the orbitals have to be reordered to perform the CAS-SCF calculation, by permuting two orbitals to begin the calculation.
- (20) Boncella, J. M.; Tilley, T. D.; Andersen, R. A. *J. Chem. Soc., Chem. Commun.* **1984**, 710–712.
- (21) Walter, M.; Berg, D. J.; Andersen, R. A. *Organometallics* **2006**, *25*, 3228–3237.
- (22) Schultz, M.; Boncella, J. M.; Berg, D. J.; Tilley, T. D.; Andersen, R. A. *Organometallics* **2002**, *21*, 460–472.
- (23) Evans, W. J.; Drummond, D. K. *J. Am. Chem. Soc.* **1989**, *111*, 3329–3335.
- (24) Veauthier, J. M.; Schelter, E. J.; Carlson, C. N.; Scott, B. L.; Da Re, R. E.; Thompson, J. D.; Kiplinger, J. L.; Morris, D. E.; John, K. D. *Inorg. Chem.* **2008**, *47*, 5841–5849.
- (25) Nocton, G.; Ricard, L. *Dalton Trans.* **2014**, DOI: 10.1039/C3DT52641K.
- (26) Jaroschik, F.; Nief, F.; Le Goff, X.-F.; Ricard, L. *Organometallics* **2007**, *26*, 3552–3558.
- (27) Namy, J. L.; Girard, P.; Kagan, H. B. *New J. Chem.* **1977**, *1*, 5–7.
- (28) Girard, P.; Namy, J. L.; Kagan, H. B. *J. Am. Chem. Soc.* **1980**, *102*, 2693–2698.
- (29) Procter, D. J.; Flowers, R. A., II; Skydstrup, T. In *Organic Synthesis Using Samarium Diodide, A Practical Guide*; Royal Society of Chemistry: London, 2010.
- (30) Molander, G. A. *Chem. Rev.* **1992**, *92*, 29–68.
- (31) Molander, G. A.; McKie, J. A. *J. Org. Chem.* **1992**, *57*, 3132–3139.

- (32) Enemærke, R. J.; Hertz, T.; Skydstrup, T.; Daasbjerg, K. *Chem.—Eur. J.* **2000**, *6*, 3747–3754.
- (33) Shabangi, M.; Flowers, R. A., II. *Tetrahedron Lett.* **1997**, *38*, 1137–1140.
- (34) Kefalidis, C. E.; Perrin, L.; Maron, L. *Eur. J. Inorg. Chem.* **2013**, 22–23, 4041–4049.
- (35) Farran, H.; Hoz, S. *Org. Lett.* **2008**, *10*, 4875–4877.
- (36) Frisch, M. J.; et al. *Gaussian 03*, Revision C.02; Gaussian, Inc.: Wallingford, CT, 2004.
- (37) (a) Becke, A. D. *J. Chem. Phys.* **1993**, *98*, 5648–5662.
(b) Perdew, J. P.; Wang, Y. *Phys. Rev. B* **1992**, *45*, 13244–13249.
- (38) (a) Dolg, M.; Stoll, H.; Preuss, H. *J. Chem. Phys.* **1989**, *90*, 1730–1734. (b) Cao, X.; Dolg, M. *THEOCHEM* **2002**, *581*, 139–147.
- (39) Bergner, A.; Dolg, M.; Kuechle, W.; Stoll, H.; Preuss, H. *Mol. Phys.* **1993**, *80*, 1431–1441.
- (40) Maron, L.; Teichtel, C. *Chem. Phys.* **1998**, *237*, 105–122.